Characterization of Highly Reductive Modification of Tetracycline D-Ring Reveals Enzymatic Conversion of Enone to Alkane

Qiu-Yue Nie
Shanghai Institute of Organic Chemistry
Zhen-Yu Ji
Shanghai Institute of Organic Chemistry
Yu Hu
Shanghai Institute of Organic Chemistry, Chinese Academy of Sciences
Gong-Li Tang (gltang@sioc.ac.cn)
Shanghai Institute of Organic Chemistry https://orcid.org/0000-0003-3149-4683

Article

Keywords: Tetracyclines, structure

Posted Date: January 18th, 2021

DOI: https://doi.org/10.21203/rs.3.rs-141868/v1

Abstract

Tetracyclines are an eminent family of type II polyketides which possess a variety of decoration on the skeletons. However, apart from the oxidative modification in aureolic acid compounds, there are few cases on the further conversion of α, β-unsaturated ketones in the tetracycline D-ring. Here, we identified two reductases (TjhO5 and TjhD4) that highly reduced the α,β-unsaturated ketone of D-ring in the biosynthesis of unconventional tetracyclines. By identifying related intermediates and conducting isotope incorporation experiments, we demonstrated that the entire transformation could be accomplished by TjhO5 and TjhD4 collectively via two distinct pathways involving different enzymatic mechanisms. A distinctive deoxygenation mechanism was possibly involved in the TjhO5-mediated continuous reduction of C = O to CH_2. These findings highlight the unprecedent post-modification of tetracyclines and facilitate further engineering to enrich the structural diversities.

Introduction

Type II polyketides belong to a structurally diverse family of natural products with various biological activities,[1–3] and are closely related to the human microbiome.[4] As an essential class of type II polyketides, tetracyclines are clinically used to treat a variety of infections.[5,6] During the biosynthesis of bacterial tetracyclines, such as tetracycline (TC), chlortetracycline (CTC), oxytetracycline (OTC), and SF2575,[7–10] the same intermediate 2,4-keto-anhydrotetracycline (ATC) can be further modified by various tailoring enzymes to obtain diverse tetracyclines (Fig. 1a and Supplementary Fig. 1a) [11–14]. Nevertheless, the α,β-unsaturated ketone of D-ring is generally retained in the final products except aureolic acid compounds including mithramycin[15–18], whose scaffolds are formed via cleaving the D-ring of tetracycline precursors through Baeyer-Villiger oxidation (Supplementary Fig. 1b).[19–22]

In recent study, we activated and characterized a silent gene cluster *tjh* in *Streptomyces aureus suzhoueusis* governing the biosynthesis of two types of type II polyketides (pentacyclic and tetracycline structures).[23] Compared with typical tetracyclines containing α,β-unsaturated ketones, the D-rings of these non-canonical tetracyclines have been highly reduced to either C = C (**5**–**7**) or C-C bond (**9**–**11**) (Fig. 1a). Considering that three new compounds (**12**–**14**) with similar core structure to 4-hydroxy-ATC have been previously identified in Δ*tjhO5* mutants, the atypical tetracyclines are likely to be converted from intermediates with α,β-unsaturated ketone (Fig. 1a and Supplementary Fig. 1a). Intuitively, the transformation of enone to alkane in D-ring can be divided into two sub-processes consisting of reduction of the C = C bond and conversion of C = O to CH_2. The strategies for reducing ketone to alkane in organic synthesis have been widely developed mainly including Wolff-Kishner-Huang reduction, Clemmensen reduction and Caglioti reduction (Fig. 1b).[24] Correspondingly, such conversion in nature mainly occurs in type I polyketides biosynthesis, which is achieved through three enzymatic domains of type I polyketide synthase (PKS) including ketoreductase (KR), dehydratase (DH) and enol reductase (ER) (Fig. 1c).[25] In this study, we found that the quinone oxidoreductase TjhO5 can mediate this continuously reductive reaction of C = O to CH_2 in vivo involving a unique deoxygenation mechanism. In addition, TjhO5 along

with a NAD(P)H-dependent epimerase TjhD4 accomplished the conversion of enone to alkane in D-ring of tetracyclines. Significantly, this process was verified to go through two different biosynthetic pathways, which involved distinct intermediates and enzymatic mechanisms based on isotope labeling experiments.

Results

Biochemical characterization of TjhO5 and identification of the product. According to BLAST analysis, TjhO5 belongs to the medium-chain reductases (MDR) superfamily and NADPH:quinone oxidoreductase subfamily; it exhibits a high similarity to GrhO7 (50% identity) whose function in griseorhodin biosynthesis is not assigned.[26,27] Since **12**–**14** can deglycosylate spontaneously and **8** (with a reduced completely D-ring) can be detected in Δ*tjhB3* (*tjhB3* encoding a glycosyltransferase), the deglycosylated compound **15** should be more reliable and suitable for further studies. We generated substantial amounts of **15** via hydrolysis of *ΔtjhO5*-fermentation broth with hydrochloric acid and confirmed its structure by analysis of NMR spectroscopy data (Supplementary Fig. 19–23). Moreover, retention time (RT) of **15** was identical to that of the deglycosylated compound in the crude extract of the double knock-out mutant *ΔtjhO5/ΔtjhB3* (Supplementary Fig. 2–3). To pinpoint its function in vitro, we purified TjhO5 from *E. coli* BL21(DE3) (Supplementary Fig. 4). Different from the control assays, LC – MS showed two new peaks whose m/z ($[M-H]^-$ = 369) was consistent with the target product **4** in the reaction mixture containing NADPH, substrate **15** and TjhO5. Surprisingly, the RT of the two peaks was different from that of **4**, the major core structure produced by wild-type (WT) (Fig. 2a).

To investigate TjhO5-catalyzed reaction, the major product **16** was purified via a large-scale enzymatic assay of TjhO5. Further, the structure of **16** was confirmed by ^1H, ^{13}C, ^1H-^1H COSY, HSQC, HMBC, and NOESY NMR spectrums (Supplementary Fig. 24–29). The structure of compound **16** is similar to that of **15**, except that its C-10 carbonyl group was reduced to CH_2, and the C-7 of **16** is the *R*-configuration instead of the *S*-configuration in **15** (Fig. 2b). These differences were revealed by the evaluation of the H-7 and H-6a coupling constants in ^1H NMR data of **15** and **16**, which were 11.1 Hz and 1.6 Hz, respectively (Fig. 2c and d). Besides, in NOESY NMR spectrums, H-7 of **16** was correlated with H_β-6, but H-7 of **15** was correlated with H_α-6 (Supplementary Fig. 5). Meanwhile, a minor product (marked with * in Fig. 2a-i) was not obtained due to its low yield and lability.

In vitro reconstitution of highly reductive modification. At this stage, it is obvious that other enzymes should participate in further transformation to generate final products starting from the α,β-unsaturated ketone intermediate. Besides *tjhO5*, gene knock-out experiments verified three genes, including *tjhC5*, *tjhD2*, and *tjhD4*, to be closely related to the post-modifications of tetracyclines.[23] Based on bioinformatic analysis, TjhC5 contains a cyclase domain; TjhD2 is an aldo-keto reductase, sharing moderate homology (33% amino acid identity) with SsfF which can reduce the C-4 carbonyl of 2,4-keto-ATC; TjhD4 belongs to the short-chain dehydrogenase (SDR) superfamily and NAD^+ dependent epimerase/dehydratase subfamily, which is most likely to participate in subsequent reduction. To verify this hypothesis, we

performed various biochemical assays on TjhD4 from *E. coli* BL21(DE3) (Supplementary Fig. 4). When intermediate **16** was incubated with TjhD4 and NAD(P)H for 10 min and LC-MS was performed on products, two new products with the same m/z ($[M-H]^-$ = 371) were detected. The major product was identified as **8** and the other was a new compound **17** (Fig. 3a i-iii). The chemical structure of **17** was elucidated by NMR spectroscopy analysis (Supplementary Fig. 30–35), and its C-9 is *R*-configuration rather than *S*-configuration in **8** (Fig. 3b). In fact, **17** could be detected in the fermentation broth of WT but was ignored previously due to low titer. Although TjhD4 could convert **16** to **8** and **17** in vitro, both were minor backbones produced by WT and could not be further converted into the predominant scaffold **4**. Also, the extract of TjhO5 reactions as substrates for TjhD4 could not afford **4**, suggesting that products of TjhO5 alone could not be transformed to **4** by TjhD4 (Supplementary Fig. 6). Accidentally, incubation of **15** with TjhO5 and TjhD4 at the same time generated trace amounts of **4**. Furthermore, adjusting the ratio of TjhO5 and TjhD4 from 3:1 to 1:3 under conditions of excess substrate **15** significantly improved the yield of **4** (Fig. 3a v-vii). Consequently, we proposed that the formation of **4** needed an optimal ration of both enzymes because excess TjhO5 might convert **4** to **8** and **17** (Fig. 3b). As expected, incubation of TjhO5, **4** and NADPH resulted in the appearance of **8** and **17**, and concomitant disappearance of **4** (Fig. 3a x-xi). These results suggested that i) either TjhO5 or TjhD4 was indispensable for transformation of the α,β-unsaturated ketone substrate **15** to **4**, **8**, and **17**; ii) TjhO5, a multifunctional enzyme, could not only reduce the ketone to CH_2 and isomerize the C-7 but also reduce different functional groups including C = O and C = C double bonds; iii) TjhD4 is a bi-functional enzyme which could catalyze epimerization and reduction reactions simultaneously; iv) the formation of **8** and **17** beginning with **15** went through two different intermediates respectively via two distinct biosynthetic pathways (path A and B) which appeared in the stepwise and one-pot reaction, respectively (Fig. 3b).

Elucidation of the enzymatic mechanisms in two distinct pathways. For an in-depth analysis of the enzymatic mechanism, the activity of TjhO5 was reconstituted in the presence of (*R*)-[4-^{2}H]-NADPH generated in situ by glucose dehydrogenase (GDH) from *Thermoplasma acidophilum* ATCC 25905 (TaGDH), using D-[1-^{2}H]-glucose as the deuterium donor.[28,29] The mass shift of + 2 Da at m/z 371 was detected in a TaGDH/TjhO5 coupled assay (Supplementary Fig. 7). We prepared ^{2}H-**16** via large-scale enzymatic reaction and ^{2}H NMR revealed that two deuteriums (δ^2H 2.48, δ^2H 2.70) were incorporated in **16** at C-10 (Fig. 4a and b). Meanwhile, enzymatic assay of TjhD4 was conducted in the presence of (*S*)-[4-^{2}H]-NADPH provided by a GDH from *Bacillus megaterium* DSM 2894 (BmGDH) using the same deuterium donor.[30] BmGDH/TjhD4 coupled assay could produce two compounds, both showing a mass increment of + 1 Da (Supplementary Fig. 8).

To identify the deuterium position, BmGDH/TjhO5/TjhD4 assay was carried out using substrate **15**. ^{1}H and ^{13}C NMR spectrums of isolated ^{2}H-**4**, ^{2}H-**8** and ^{2}H-**17** showed that H-8 was replaced by one deuterium (Fig. 4c, Supplementary Fig. 9–10, and 43–48). These results proved that TjhO5 reduced **15** twice at C-10 and TjhD4 reduced substrates once at C-8.

Given that the configuration of C-7 was reversed in TjhO5-governed reaction in path A, we proposed that there were two plausible catalytic mechanisms for forming **16**. TjhO5 firstly reduced the carbonyl of C-10 to hydroxy resulting in compound **18** (Supplementary Fig. 11a). In one of the hypotheses, **18** was then dehydrated and tautomerized to form the intermediate **20**, which could be transformed to **16** by 1,4-addition. Alternatively, **19** could be reduced to intermediate **21**, which subsequently went through four times of enol interconversions to form **16**. To confirm the mechanism, we introduced enzymatic reactions in D_2O at first. The mass data of **16** did not change revealed by LC-MS, suggesting the reaction did not abstract the proton from water to C-7 (Supplementary Fig. 11b). Therefore, these mechanisms which require the incorporation of a solvent-derived proton into products were invalidated.[31,32] Since the oxygen of carbonyl in β-hydroxyl-α,β-enone was easily exchanged with water oxygen,[33] the incubation of **15** and $H_2{}^{18}O$ resulted in the mass increment in + 2 Da and + 4 Da, indicating that both oxygens of **15** in C-10 and C-13 could exchange with $H_2{}^{18}O$ (Supplementary Fig. 12). After the reaction of TjhO5 in $H_2{}^{18}O$ went to completion, the MW of **16** increased in + 2 and + 4. Then, **16** were extracted from the solvent and re-equilibrated in $H_2{}^{16}O$ overnight, after which we still observed a + 2 increase in MW of **16** (Fig. 5b and Supplementary Fig. 13). These results suggested that oxygen of C-10 was retained in this reaction and might migrate to C-7. We proposed that the deoxygenation was possibly achieved via generating a potential cyclic ether intermediate in the virtue of acid residues (Fig. 5a), reminiscent of acid-mediated cyclic ether formation in platensimycin biosynthesis.[34] After completion of the TjhO5 reaction in $H_2{}^{18}O$, TjhD4 was added to afford **8** and **17**, whose MW still increased by + 2 and + 4 (Supplementary Fig. 14). However, when simultaneously incubating TjhO5, TjhD4, NADPH and **15** in $H_2{}^{18}O$, we detected only + 2 increase in MW of all products, suggesting that path A and path B involved different enzymatic mechanisms (Fig. 3b and Supplementary Fig. 14). Furthermore, in the one-pot reaction with D_2O, MW of **8** and **17** increased 1 Da, while the MW of **4** did not change significantly revealed by LC-MS (Supplementary Fig. 15). These results verified that the formation of **4** did not require oxygen transfer, as well as abstraction of a proton from water to carbon. Therefore, in the co-incubation of TjhD4 and TjhO5, H^- provided by TjhD4 rapidly attacked **18** to afford **4** (Supplementary Fig. 15), which could be further reduced by TjhO5 to yield **8** and **17**.

Discussion

We successfully reconstituted the highly reductive modification of tetracycline D-ring by TjhO5 and TjhD4 in vitro, involving two different biosynthetic pathways with distinct enzymatic mechanisms (Fig. 6). In path A, TjhO5 reduces the carbonyl group of C-10 to hydroxy to form the potential intermediate **22**, which can be reduced by TjhO5 again to produce **16**. TjhD4 could epimerize C-7 and reduce C-8 to form **8** and **17**. The enzymatic function of reducing double bond or deoxygenation has been well studied. Significantly, it is rarely reported that one reductase is responsible for the conversion of C = O to CH_2, because such transformation usually involves multi-step reduction and deoxygenation. More interestingly, the C-10 deoxygenation characterized in this study is inherently mechanistically different from dehydration catalyzed by KstA10 in kosinostatin biosynthesis [35], radical mechanism in apramycin,

IPP and DMAPP biosynthesis[36, 37], and α-carbonyl mediated mechanism guided by the PMP-dependent enzyme SpnQ in D-forosamine biosynthesis[38] (Supplementary Fig. 16a-d). TjhO5 may remove a hydroxy of C-10 via the oxygen transfer mechanism, accompanying hydroxy isomerization. Moreover, TjhD4 belongs to the NADH-dependent epimerases, which usually participate in deoxysugar biosynthesis and exploit the enol interconversion of α-carbonyl to isomerize (Supplementary Fig. 16e).[39,40] Although the catalytic mechanism of homologous enzymes has been well elucidated, to our knowledge, it has not been reported that this enzyme can conduct reduction and isomerization on the backbone of type II polyketides. In path B, two enzymes are required to work coordinately in the first step. After TjhO5 reduces the carbonyl of C-10, TjhD4 rapidly catalyzes the attack of H^- at C-8 of **18**, resulting in the disappearance of hydroxy to produce **4**, which is reduced to **8** and **17** by TjhO5 again (Fig. 6). TjhO5 may exhibit a jumping catalytic mode in this pathway rather than a continuous catalytic mode in path A. In addition, the phenomenon that the same products are formed through two different pathways with distinct intermediates from a common substrate is rare.[41] Consequently, TjhO5 and TjhD4 both exhibit high catalytic promiscuity in these two pathways.

The sequence similarity network (SSN) analysis of TjhO5 revealed that the group closely related to TjhO5 is different from most quinone oxidoreductases (Supplementary Fig. 17). More specifically, proteins with high homology to TjhO5 are extensively involved in the biosynthesis of type II polyketides, such as GrhO7, MsnO9 and HrsP2, which are related to the biosynthesis of griseorhodin, mensacarcin and hiroshidine respectively (Supplementary Fig. 18).[26,42,43] Although quinone oxidoreductases are commonly involved in type II polyketides biosynthesis, the functions of most of these proteins remains to be fully determined. This study lays the foundation for functional characterization of these enzymes.

In summary, we identified two enzymes that could cooperatively reduce a D-ring with α,β-unsaturated ketone to a saturated D-ring via two distinct pathways with different enzymatic mechanisms. This study highlights the reactive diversity of reductases and sheds light on the role of quinone oxidoreductases and epimerases in the biosynthesis of type II polyketides, which can be applied in genome mining, biocatalysis and combinatorial biosynthesis.

Methods

General. Specific bacterial strains and plasmids used in this study were summarized in Table S1, PCR primers were listed in Table S2. General enzymes, chemicals, Kits, media, and molecular biological reagents were from standard commercial sources. Bioinformatics analysis, DNA isolation, manipulation, construction of gene replacement and complementation mutants were preformed following the standard methods.

Large Scale Fermentation, Isolation of Metabolites from *S. aureus suzhoueusis* SP-371 Mutant Strains. *S. aureus suzhoueusis* TG6004 were grown in TSB (tryptic soy broth) (3%) at 30 °C for 24 h as a seed culture, then 5 mL of seeding culture suspension was transferred into a 500-mL flask containing 100 mL

fermentation broth (1% soy bean, 1% peanut meal, 5% glucose, 2% corn starch, 0.6% NH_4NO_3, 0.3% NaCl, 0.6% $CaCO_3$, pH = 7.2) and the flask was cultured at 30 ℃and 220 rpm for an additional 5 d.

Hydrolysis of fermentation broth. The fermentation broth of Δ*tjhO5*::*2R* (TG6027) was dissolved by suitable amount of methanol with 0.25 M hydrochloric acid at 25 ℃ stirring for 1–3 h.

Construction of double knockout mutant Δ tjhO5 **/** B3. The plasmid TG6018 was introduced from *E. coli* S17-1 into *S. aureus suzhoueusis* SP-371 and apramycin-resistant clones were screened at 30 ℃. After picking candidate exconjugants to obtain single-crossover mutants in TSB (tryptic soy broth, 3%) liquid medium with apramycin at 37 ℃, the single-crossover mutants were grown in TSB without antibiotics. The double knockout mutants *S. aureus suzhoueusis* Δ*tjhO5*/ *tjhB3* (*S. aureus suzhoueusis* TG6032) were confirmed by PCR using TjhB3-yz-f/r as primers (Table S2).

Enzymatic assays and metabolite analysis. High performance liquid chromatography (HPLC) analysis was conducted on Thermo Scientific Dionex Ultimate 3000 (Thermo Fisher Scientific Inc., USA) with a reverse-phase Alltima C18 column (5 μm, 4.6×250 mm). Semi-preparative HPLC was performed on a Shimadzu LC-20-AT system using an YMC-Pack ODS column (YMC, 250×10 mm, 5 μm). HPLC electrospray ionization MS (HPLC-ESI-MS) was performed on the Thermo Fisher LTQ Fleet ESI-MS spectrometer (Thermo Fisher Scientific Inc., USA). High-resolution ESI-MS analysis was conducted on the 6230B Accurate Mass TOF LC/MS System (Agilent Technologies Inc., USA).

HPLC analysis was carried out on a HPLC was performed using a reverse-phase Alltima C18 column (5 μm, 4.6×250 mm) with UV detection at 270 nm. The column was equilibrated with 76% solvents A (H_2O and 0.1% HCOOH) and 24% B (MeCN and 0.1% HCOOH) and developed with the following program: T = 0 min, 24% B; T = 24 min, 60% B; T = 29 min, 80% B; T = 30 min, 95% B; T = 33 min, 95% B; T = 35 min, 24% B, with a flow rate of 1 mL/min.

Protein Expression and purification. The *TjhO5* gene was amplified by PCR from genome DNA using the primers shown in Table S2. The purified PCR products were ligated to pMD19-T and confirmed by sequencing. The code of *TjhD4* was optimized and this gene was synthesized and cloned into pUC57 by Genewiz. The *Nde*I/*Hind*III fragment was cloned into the same sites of pET28a to yield plasmid pTG6032 (*TjhO5*) and pTG6033 (*TjhD4*), in which enzyme will be overproduced as a C-terminal 8x His-tagged fusion protein. For TjhO5 and TjhD4 expression and purificatin, plasmid pTG6032 and pTG6033 was transformed respectively into BL21(DE3) competent *Escherichia coli* cells which were grown at 37 ℃ in 800 mL LB with 50 μg/mL kanamycin to an OD600 of 0.6–0.8. Then the cells were induced with 0.1 mM IPTG for 20 hr at 16 ^{o}C. The cells were harvested by centrifugation (4,000 rpm, 8 min) and resuspended in 35 mL of Tris buffer (50 mM Tris, pH 8.0, 100 mM NaCl) and lysed by ultrasonication on ice. The lysates were clarified by centrifugation (30 min, 16,500 rpm), and the His-tagged fusion proteins were purified with nickel-affinity chromatography though a linear gradient of 25–500 mM imidazole in the lysis buffer. The fractions were collected in a buffer containing 50 mM Tris, pH 8.0, and 50 mM NaCl. Proteins were

analysed by SDS-PAGE gels. Finally, their concentrations were estimated from the absorbance at 280 nm with their corresponding absorption coefficients.

Enzymatic assay.

1) The enzymatic assay of TjhO5 using **15** was carried out at 30 ℃ in a 50 µl aliquot containing 50 mM Tris-HCl (pH 8.0), 10 µM TjhO5, 1 mM NADPH, 0.2 mM **15**. After 30 min, the assay was quenched by 50 µl MeOH.

2) The enzymatic assay of TjhD4 using **16** was carried out at 30 ℃ in a 50 µl aliquot containing 50 mM Tris-HCl (pH 8.0), 5 µM TjhD4, 0.5 mM NADH, 0.1 mM **16**. After 10 min, the assay was quenched by 50 µl MeOH.

3) The enzymatic assay of TjhO5 and TjhD4 using **15** was carried out at 30 ℃ in a 50 µl aliquot containing 50 mM Tris-HCl (pH 8.0), 5 µM TjhD4, 10 µM TjhO5, 0.5 mM NADPH, 0.2 mM **15**. Under the condition of 0.4 mM **15**, the specific concentrations in the experiments of changing ratio of TjhO5 and TjhD4: (1) 15 µM TjhD4 and 5 µM TjhO5; (2) 10 µM TjhD4 and 10 µM TjhO5; (3) 5 µM TjhD4 and 15 µM TjhO5. After 1 h, these assays were quenched by 50 µl MeOH. 4) The enzymatic assay of TjhO5 using **4** was carried out at 30 ℃ in a 50 µl aliquot containing 50 mM Tris-HCl (pH 8.0), 5 µM TjhO5, 1 mM NADPH, 0.1 mM **4**. After 30 min, this assay was quenched by 50 µl MeOH.

4) In the enzymatic assay of TjhO5/TaGDH or BmGDH, 50 mM Tris-HCl (pH 8.0), 1 mM $NADP^+$, 10 mM D-[1-^{2}H]-glucose, 10 µM BmGDH or TaGDH was incubated in 37 ℃ for 30 min, and then after making the reaction cool down to 30 ℃, added TjhO5 and **15** to 5 µM and 0.1 mM respectively.

5) In the enzymatic assay of TjhD4/TaGDH or BmGDH, 50 mM Tris-HCl (pH 8.0), 1 mM $NADP^+$, 10 mM D-[1-^{2}H]-glucose, 10 µM BmGDH or TaGDH was incubated in 37 ℃ for 30 min, and then after making the reaction cool down to 30 ℃, added TjhD4 and **16** to 2.5 µM and 0.025 mM respectively.

6) In the enzymatic assay of TjhO5 with $H_2{}^{18}O$. **15** was incubated in 50 µL 97% $H_2{}^{18}O$ for 30 min in 37 ℃. Then after making the reaction cool down to 30 ℃, TjhO5, NADPH and Tris-HCl Buffer were incubated in 30 ℃ for 30 min. The enzymatic reactions were extracted by equal amount of CH_2Cl_2, centrifuged at 12,000 g for 5 min. The organic phase was evaporated and added 5 µL DMSO and 100 µL H_2O for overnight.

Large scale preparation of enzymatic products.

1) **16**: A 10 mL reaction contain 50 mM Tris-HCl (pH 8.0), 10 µM TjhO5, 2 mM NADPH, 0.2 mM **15**. The solution was extracted by CH_2Cl_2. The crude extracts were purified by semi-preparative HPLC with isocratic elution by acetonitrile and water using a flow rate of 3 mL/min (50% acetonitrile).

2) ^{2}H-**16**: 500 μL x100 reaction contain 50 mM Tris-HCl (pH 8.0), 2 mM $NADP^{+}$, 20 mM D-[1-^{2}H]-glucose, 20 μM TaGDH incubated in 37 ℃ for 1 h, and then after making the reaction cool down to 30 ℃, added TjhO5 and **15** to 10 μM and 0.25 mM respectively. The solution was extracted by CH_2Cl_2. The crude extracts were purified by semi-preparative HPLC with isocratic elution by acetonitrile and water using a flow rate of 3 mL/min (50% acetonitrile).

3) ^{2}H-**4**, ^{2}H-**8**, and ^{2}H-**17**: 500 μL x200 reaction contain 50 mM Tris-HCl (pH 8.0), 2 mM $NADP^{+}$, 20 mM D-[1-^{2}H]-glucose, 20 μM BmGDH incubated in 37 ℃ for 1 h, and then after making the reaction cool down to 30 ℃, added TjhO5, TjhD4 and **15** to 5 μM, 10 μM and 0.25 mM respectively. The solution was extracted by ethyl acetate. The crude extracts were purified by semi-preparative HPLC with isocratic elution by acetonitrile and water using a flow rate of 3 mL/min (30% acetonitrile).

Analytical Data.

Compound 15. yellow solid; HR-ESI-MS (-) found m/z 383.0781 $[M-H]^-$ (calcd $[M-H]^-$ for $C_{20}H_{15}O_8$, 383.0772); NMR data see Supplementary Table 3 and Supplementary Fig. 19–23.

Compound 16. yellow solid; HR-ESI-MS (-) found m/z 369.0990 $[M-H]^-$ (calcd $[M-H]^-$ for $C_{20}H_{17}O_7$, 369.0980); NMR data see Supplementary Table 4 and Supplementary Fig. 24–29.

Compound 17. yellow solid; HR-ESI-MS (-) found m/z 371.1145 $[M-H]^-$ (calcd $[M-H]^-$ for $C_{20}H_{19}O_7$, 371.1136); NMR data see Supplementary Table 5 and Supplementary Fig. 30–35.

Compound 4. yellow solid; HR-ESI-MS (-) found m/z 369.0989 $[M-H]^-$ (calcd $[M-H]^-$ for $C_{20}H_{17}O_7$, 369.0980); NMR data see Supplementary Table 6 and Supplementary Fig. 36–41.

Compound ^{2}H-16. yellow solid; HR-ESI-MS (-) found m/z 371.1112 $[M-H]^-$ (calcd $[M-H]^-$ for $C_{20}H_{15}{}^{2}H_2O_9$, 371.1105); NMR data see Supplementary Fig. 42.

Compound ^{2}H-4. yellow solid; HR-ESI-MS (-) found m/z 370.1051 $[M-H]^-$ (calcd $[M-H]^-$ for $C_{20}H_{16}{}^{2}H_2O_7$, 370.1043); NMR data see Supplementary Fig. 43–44.

Compound ^{2}H-8. yellow solid; HR-ESI-MS (-) found m/z 372.1208 $[M-H]^-$ (calcd $[M-H]^-$ for $C_{20}H_{18}{}^{2}H_2O_9$, 372.1199); NMR data see Supplementary Fig. 45–46.

Compound ^{2}H-17. yellow solid; HR-ESI-MS (-) found m/z 372.1210 $[M-H]^-$ (calcd $[M-H]^-$ for $C_{20}H_{15}{}^{2}H_2O_9$, 372.1199); NMR data see Supplementary Fig. 47–48.

Declarations

Acknowledgements

We thank Prof. Han-Jie Ying in Nanjing University of Technology for providing the plasmid pRSF-BmGDH; Prof. Chang-Sheng Zhang of South China Sea Institute of Oceanology, CAS, for kindly giving us pCSG3622. This work was financially supported by grants from National Natural Science Foundation of China (21632007 and 21621002) and CAS (XDB20000000 and K. C. Wong Education Foundation).

References

1. Hertweck, C. The biosynthetic logic of polyketide diversity. *Chem. Int. Ed*. **48**, 4688-4716 (2009).
2. Rawlings, B. J. Biosynthesis of polyketides (other than actinomycete macrolides), *Nat. Prod. Rep*. **16**, 425-484 (1999).
3. Das, A.; Khosla, C. Biosynthesis of aromatic polyketides in bacteria. *Acc. Chem. Res*. **42**, 631-639 (2009).
4. Sugimoto, Y.; Camacho, F. R.; Wang, S.; Chankhamjon, P.; Odabas, A.; Biswas, A.; Jeffrey, P. D.; Donia, M. S. A metagenomic strategy for harnessing the chemical repertoire of the human microbiome. *Science* **366**, eaax9176 (2019).
5. Roberts, M. C. Tetracycline therapy: update. *Infect. Dis.* **36**, 462-467 (2003).
6. Griffin, M. O.; Fricovsky, E.; Ceballos, G.; Villarreal, F. Tetracyclines: a pleitropic family of compounds with promising therapeutic properties. Review of the literature*. Am. J. Physiol.: Cell Physiol.* **299**, C539-C548 (2010).
7. Hertweck, C.; Luzhetskyy, A.; Rebets, Y.; Bechthold, A. Type II polyketide synthases: gaining a deeper insight into enzymatic teamwork. *Prod. Rep.* **24**, 162-190 (2007).
8. Finlay, A. C.; Hobby, G. L.; P'an, S. Y.; Regna, P. P.; Routien, J. B.; Seeley, D. B.; Shull, G. M.; Sobin, B. A.; Solomons, I. A.; Vinson, J. W.; Kane, J. H. Terramycin, a new antibiotic. *Science* **111**, 85 (1950).
9. Hatsu, M.; Sasaki, T.; Watabe, H.; Miyadoh, S.; Nagasawa, M.; Shomura, T.; Sezaki, M.; Inouye, S.; Kondo, S. A new tetracycline antibiotic with antitumor activity. Taxonomy and fermentation of the producing strain, isolation and characterization of SF2575. *J. Antibiot*. **45**, 320-324 (1992).
10. Hatsu, M.; Sasaki, T.; Gomi, S.; Kodama, Y.; Sezaki, M.; Inouye, S.; Kondo, S. The structural elucidation of SF2575. *J. Antibiot*. **45**, 325-330 (1992).
11. Pickens, L. B.; Kim, W.; Wang, P.; Zhou, H.; Watanabe, K.; Gomi, S.; Tang, Y. Biochemical analysis of the biosynthetic pathway of an anticancer tetracycline SF2575. *Am. Chem. Soc.* **131**, 17677-17689 (2009).
12. Wang, P.; Kim, W.; Pickens, L. B.; Gao, X.; Tang, Y. Heterologous expression and manipulation of three tetracycline biosynthetic pathways. *Chem. Int. Ed*. **51**, 11136-11140 (2012).
13. Lešnik, U.; Lukežič, T.; Podgoršek, A.; Horvat, J.; Polak, T.; Šala, M.; Jenko, B.; Harmrolfs, K.; Ocampo-Sosa, A.; Martínez-Martínez, L.; Herron, P. R.; Fujs, Š.; Kosec, G.; Hunter, I. S.; Müller, R.; Petković, H.

Angew. Chem. Int. Ed. **54**, 3937-3940 (2015).

14. Wang, P.; Bashiri, G.; Gao, X.; Sawaya, M. R.; Tang, Y. Uncovering the enzymes that catalyze the final steps in oxytetracycline biosynthesis. *Am. Chem. Soc.* **135**, 7138-7141 (2013).
15. Grundy, W. E.; Goldstein, A. W.; Rickher, C. J.; Hanes, M. E.; Warren, H. B. J.; Sylvester, J. C. Aureolic acid, a new antibiotic. I. Microbiological studies. *Chemother.* **3**, 1215-1221 (1953).
16. Berlin, Y. A.; Esipov, S. E.; Kolosov, M. N.; Shemyakin, M. M. The structure of the olivomycin-chromomycin antibiotics (from Streptomyces olivoreticuli). *Tetrahedron Lett.* **15**, 1643-1647 (1966).
17. Yoshimura, Y.; Koenuma, M.; Matsumoto, K.; Tori, K.; Terui, Y. NMR studies of chromomycins, olivomycins, and their derivatives. *Antibiot.* **41**, 53-67 (1988).
18. Jayasuriya, H.; Lingham, R. B.; Graham, P.; Quamina, D.; Herranz, L.; Genilloud, O.; Gagliardi, M.; Danzeisen, R.; Tomassini, J. E.; Zink, D. L.; Guan, Z. S.; Singh, B. *J. Nat. Prod.* **65**, 1091-1095 (2002).
19. Prado, L.; Fernández, E.; Weißbach, U.; Blancol, G.; Quirós, L. M.; Braña, A. F.; Méndez, C.; Rohr, J.; Salas, J. A. Oxidative cleavage of premithramycin B is one of the last steps in the biosynthesis of the antitumor dtrug mithramycin. *Biol.* **6**, 19-30 (1999).
20. Bosserman, M. A.; Downey, T.; Noinaj, N.; Buchanan, S. K.; Rohr, Molecular insight into substrate recognition and catalysis of Baeyer-Villiger monooxygenase MtmOIV, the key frame-modifying enzyme in the biosynthesis of anticancer agent mithramycin. *ACS Chem. Biol.* **8**, 2466-2477 (2013).
21. Gibson, M.; Nur-e-alam, M.; Lipata, F.; Oliveira, M. A.; Rohr, J. Characterization of kinetics and products of the Baeyer-Villiger oxygenase MtmOIV, the key enzyme of the biosynthetic pathway toward the natural product anticancer drug mithramycin from *Streptomyces argillaceus*. *Am. Chem. Soc.* **127**, 17594-17595 (2005).
22. Beam, M. P.; Bosserman, M. A.; Noinaj, N.; Wehenkel, M.; Rohr, J. Crystal structure of Baeyer-Villiger monooxygenase MtmOIV, the key enzyme of the mithramycin biosynthetic pathway. *Biochemistry* **48**, 4476-4487 (2009).
23. Ji, Z.-Y.; Nie, Q.-Y.; Yin, Y.; Zhang, M.; Pan, H.-X.; Hou, X.-F.; Tang, G.-L. Activation and characterization of cryptic gene cluster: two series of aromatic polyketides biosynthesized by divergent pathways. *Angew. Chem. Int. Ed.* **58**, 18046-18054 (2019).
24. Burton, J. W. Reduction of C=X to CH_2. *Comprehensive Organic Synthesis II*, **8**, 446-478 (2014).
25. Fischbach, M. A.; Walsh, C. T. Assembly-line enzymology for polyketide and nonribosomal peptide antibiotics: logic, machinery, and mechanisms. *Chem. Rev.* **106**, 3468-3496 (2006).
26. Yunt, Z.; Reinhardt, K.; Li, A.; Engeser, M.; Dahse, H.-M.; Gütschow, M.; Bruhn, T.; Bringmann, G.; Piel, J. Cleavage of four carbon-carbon bonds during biosynthesis of the griseorhodin A spiroketal pharmacophore. *Am. Chem. Soc.* **131**, 2297-2305 (2009).
27. Lackner, G.; Schenk, A.; Xu, Z.; Reinhardt, K.; Yunt, Z. S.; Piel, J.; Hertweck, C. Biosynthesis of pentangular polyphenols: deductions from the benastatin and griseorhodin pathways. *Am. Chem. Soc.* **129**, 9306-9312 (2007).

28. Zhang, G.; Zhang, W.; Zhang, Q.; Shi, T.; Ma, L.; Zhu, Y.; Li, S.; Zhang, H.; Zhao, Y.-L.; Shi, R.; Zhang, C. Mechanistic insights into polycycle formation by reductive cyclization in ikarugamycin biosynthesis. *Chem. Int. Ed.* **53**, 4840-4844 (2014).
29. Su, J.; Wang, Q.; Feng, J.; Zhang, C.; Zhu, D.; Wei, T.; Xu, W.; Gu, L. Engineered *Thermoplasma acidophilum* factor F3 mimics human aminopeptidase N (APN) as a target for anticancer drug development. *Med. Chem*. **19**, 2991-2996 (2011).
30. Ye, Q.; Cao, H.; Yan, M.; Cao, F.; Zhang, Y.; Li, X.; Xu, L.; Chen, Y.; Xiong, J.; Ouyang, P.; Ying, H. Construction and co-expression of a polycistronic plasmid encoding carbonyl reductase and glucose dehydrogenase for production of ethyl (S)-4-chloro-3-hydroxybutanoate. *Technol.* **101**, 6761-6767 (2010).
31. Parker, J. B.; Walsh, C. T. Stereochemical outcome at four stereogenic centers during conversion of prephenate to tetrahydrotyrosine by BacABGF in the bacilysin pathway. *Biochemistry* **51**, 5622-5632 (2012).
32. Nakano, S.; Sakane, W.; Oinaka, H.; Fujimoto, Y. Biosynthesis of acaterin: Mechanism of the reaction catalyzed by dehydroacaterin reductase. *Med. Chem*. **14**, 6404-6408 (2006).
33. Bat-Erdene, U.; Kanayama, D.; Tan, D.; Turner, W. C.; Houk, K. N.; Ohashi, M.; Tang, Y. Iterative catalysis in the biosynthesis of mitochondrial complex II inhibitors harzianopyridone and atpenin B. *Am. Chem. Soc.* **142**, 8550-8554 (2020).
34. Rudolf, J. D., Dong, L.-B.; Zhang, X. Renata, H.; Shen, B. Cytochrome P450-catalyzed hydroxylation initiating ether formation in platensimycin biosynthesis. *Am. Chem. Soc.* **140**, 12349-12353 (2018).
35. Zhang, Z.; Gong, Y.-K.; Zhou, Q.; Hu, Y.; Ma, H.-M.; Chen, Y.-S.; Igarashi, Y.; Pan, L.; Tang, G.-L. Hydroxyl regioisomerization of anthracycline catalyzed by a four-enzyme cascade. *Natl. Acad. Sci. USA.* **114**, 1554-1559 (2017).
36. Lv, M.; Ji, X.; Zhao, J.; Li, Y.; Zhang, C.; Su, L.; Ding, W.; Deng, Z.; Yu, Y.; Zhang, Q. Characterization of a C3 deoxygenation pathway reveals a key branch point in aminoglycoside biosynthesis. *J. Am. Chem. Soc*. **138**, 6427-6435 (2016).
37. Wang, W.; Wang, K.; Span, I.; Jauch, J.; Bacher, A.; Groll, M.; Oldfield, E. Are free radicals involved in IspH catalysis? An EPR and crystallographic investigation. *J. Am. Chem. Soc*. **134**, 11225-11234 (2012).
38. Hong, L.; Zhao, Z.; Liu, H.-W. Characterization of SpnQ from the spinosyn biosynthetic pathway of saccharopolyspora spinosa: mechanistic and evolutionary implications for C-3 deoxygenation in deoxysugar biosynthesis. *J. Am. Chem. Soc*. **128**, 14262-14263 (2006).
39. Graninger, B. Nidetzky, D. E. Heinrichs, C. Whitfield, P. Messner, Characterization of dTDP-4-dehydrorhamnose 3,5-epimerase and dTDP-4-dehydrorhamnose reductase, required for dTDP-L-rhamnose biosynthesis in *Salmonella enterica* serovar typhimurium LT2 *J. Biol. Chem*. **274**, 25069-25077 (1999).
40. Yan, Y.; Yang, J.; Wang, L.; Xu, D.; Yu, Z.; Guo, X.; Horsman, G. P.; Lin, S.; Tao, M.; Huang, S.-X. Biosynthetic access to the rare antiarose sugar *via* an unusual reductase-epimerase. *Sci*. **11**, 3959-

3964 (2020).

41. Du, -L.; Higgins, M. A.; Ryan, K. S. Convergent biosynthetic transformations to a bacterial specialized metabolite. *Nat. Chem. Biol.* **15**, 1043-1048 (2019).
42. Maier, S.; Heitzler, T.; Asmus, K.; Brötz, E.; Hardter, U.; Hesselbach, K.; Paululat, T.; Bechthold, A. Functional characterization of different ORFs including luciferase-like monooxygenase genes from the mensacarcin gene cluster. *ChemBioChem* **16**, 1175-1182 (2015).
43. Moon, K.; Xu, F.; Zhang, C.; Seyedsayamdost, M. R. Bioactivity-HiTES unveils cryptic antibiotics encoded in Actinomycete bacteria. *ACS Chem. Biol.* **14**, 767-774 (2019).

Figures

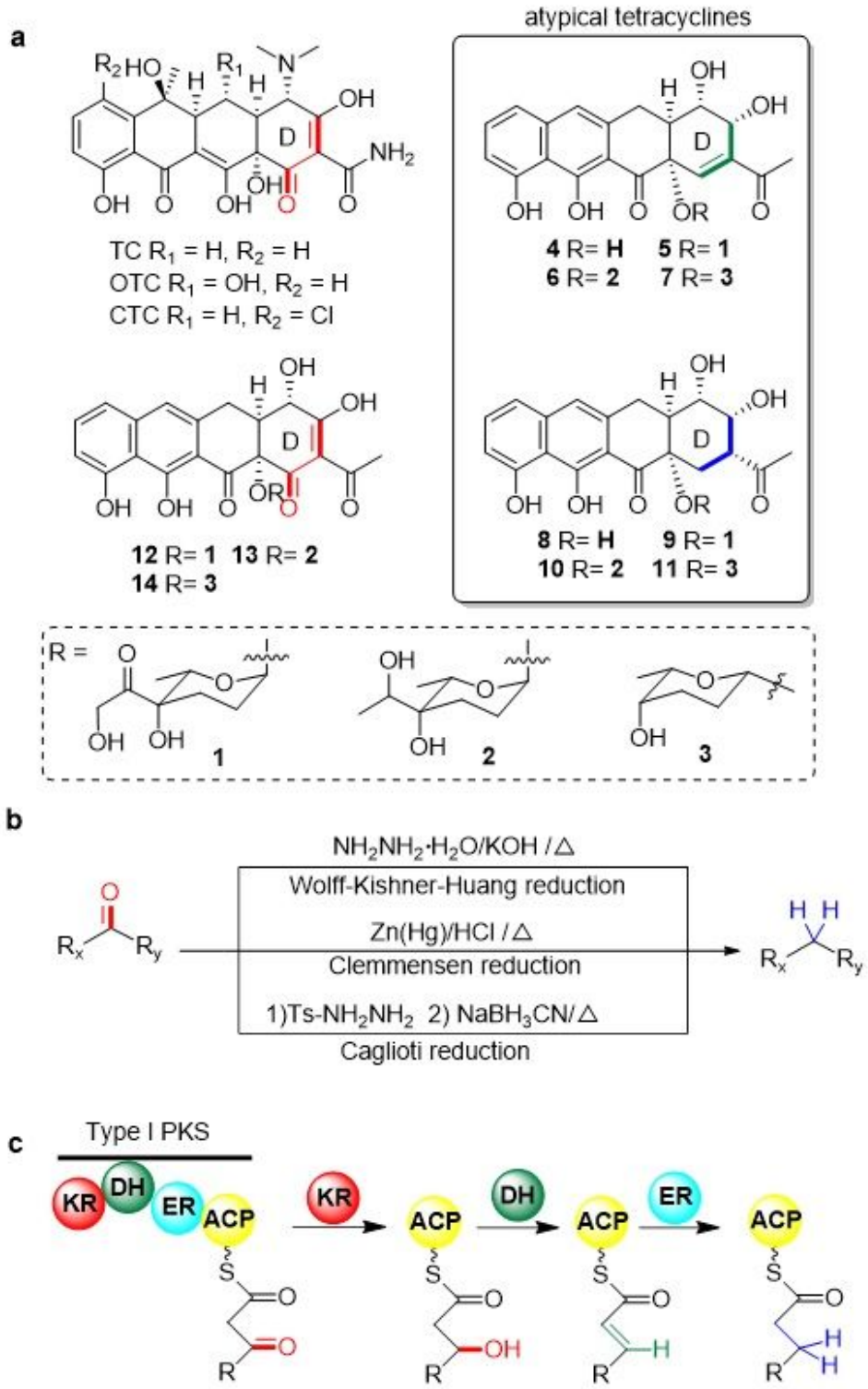

Figure 1

Chemical structures of tetracycline family natural products and reactions about reducing ketone to alkane in organic synthesis or biosynthesis. a. Chemical structures of well-known tetracyclines and atypical tetracyclines produced by Streptomyces aureus suzhoueusis. b. Chemical reactions about conversion form ketone to alkane. c. The conversion of ketone to alkane by Type I PKS. KR, ketoreductase domain; DH, dehydratase domain; ER, enol reductase domain; ACP, acyl carrier protein.

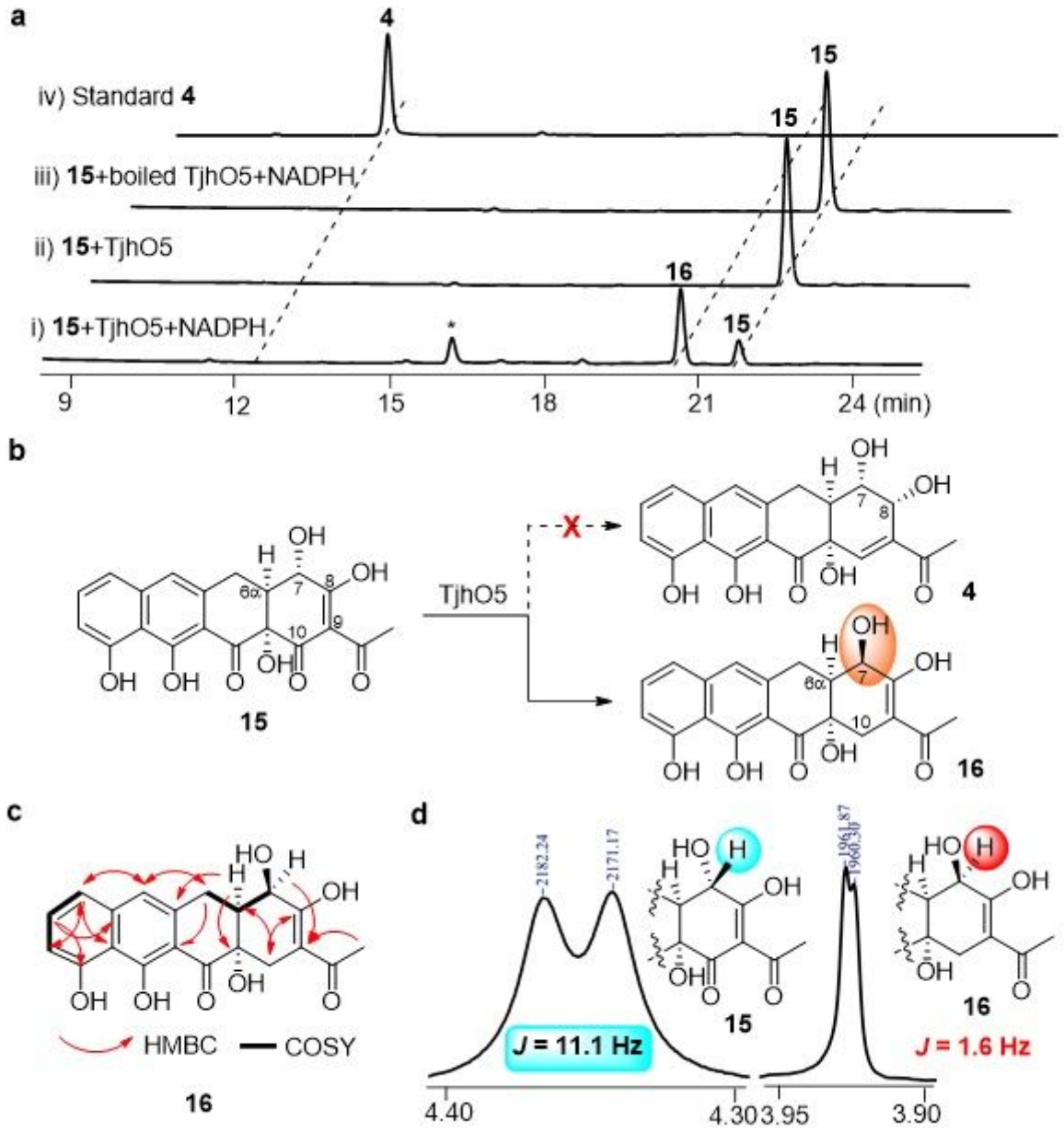

Figure 2

Characterization of TjhO5-catalysed reaction using 15 as substrate. a. HPLC analysis of enzymatic reactions with UV detected at 272 nm. The assays were conducted at 30 ºC for 30 min. b. Reaction pathway by TjhO5. c. NMR analysis of 16. d. Coupling constant of H7 and H6α in 1H NMR spectrum of 15 and 16, respectively.

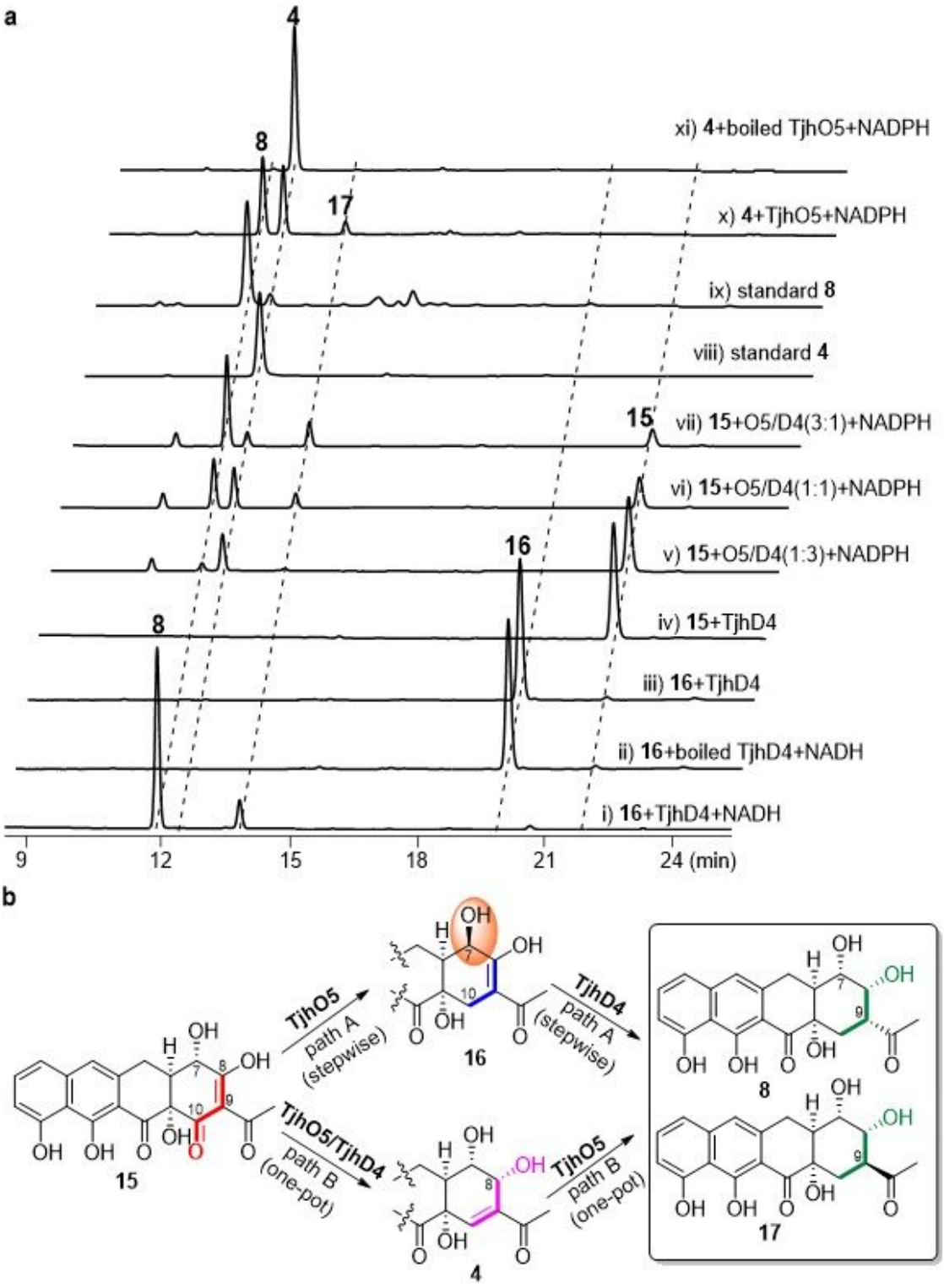

Figure 3

Functional verification of tjhD4 and in vitro reconstitution of the highly reductive modification pathways. a. HPLC analysis of enzymatic assays of TjhO5 and TjhD4 with UV detected at 272 nm. b. Proposed biosynthetic pathways including path A and B in present of stepwise and one-pot reaction respectively. Different intermediats (16 and 4) were involved in two pathways.

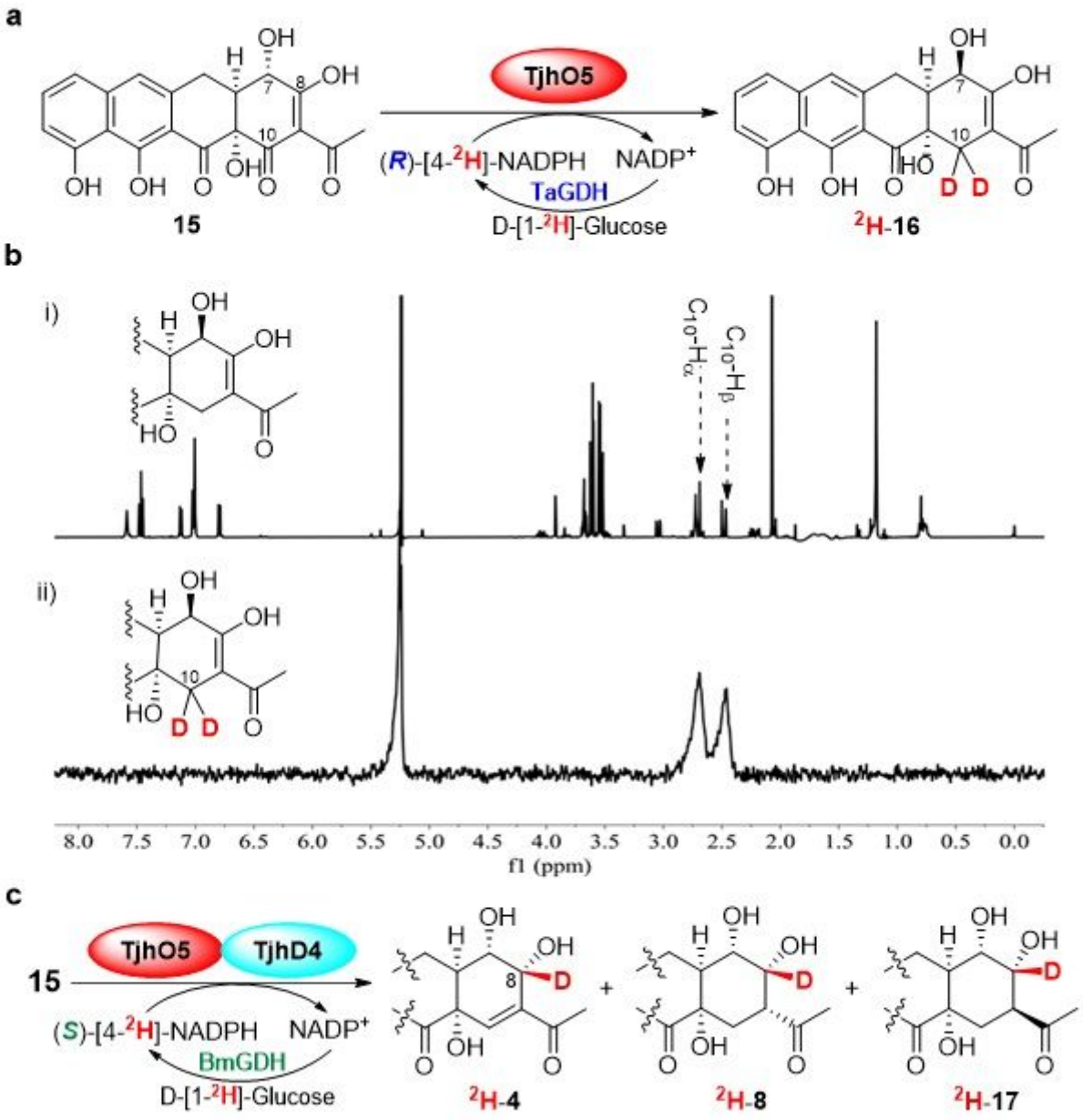

Figure 4

Biochemical assay of TjhO5 and TjhD4 with NAD(P)H regeneration and D-[1-2H]-Glucose. a. Biochemical reaction of TjhO5/TaGDH using 15 as a substrate can generate 2H-16. b. The chemical structure of 2H-16 revealed by 2H-NMR signals in CH2Cl2. i) 1H NMR spectrum of 16; ii) 2H NMR spectrum of 2H-16. c. Reaction of TjhO5/D4/BmGDH using 16 as a substrate produced 2H-4, 2H-8, and 2H-17.

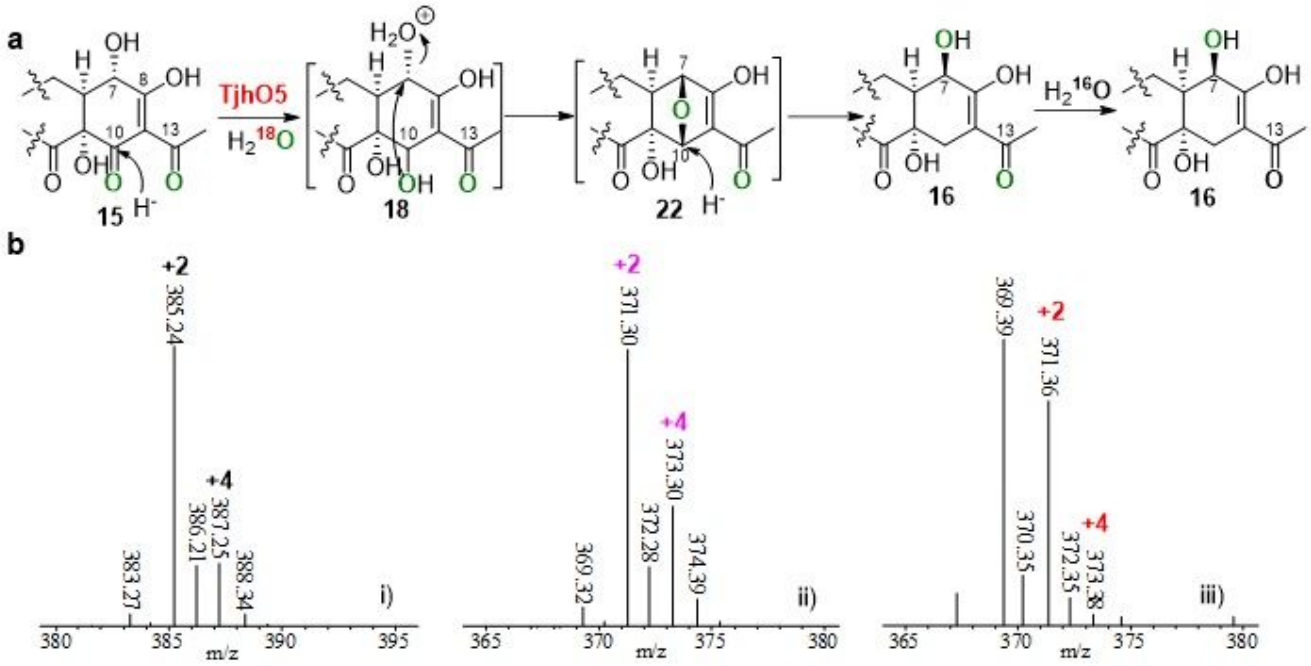

Figure 5

Enzymatic assays of TjhO5 with H18O a. Proposed enzymatic mechanisms of forming 16 via cyclic ether ring intermediate 22 by TjhO5. Oxygens coloured in green might come from H218O. b. i) Mass data of 15 after incubating in H218O at 37 ºC for 1 h; ii) Mass data of 16 produced by adding TjhO5 after incubating 15 with H218O; iii) Mass data of 16 extracted from the reaction in H218O and re-equilibrated in H216O overnight (When the incubation time in H216O was extended, the mass spectrometry data remained unchanged).

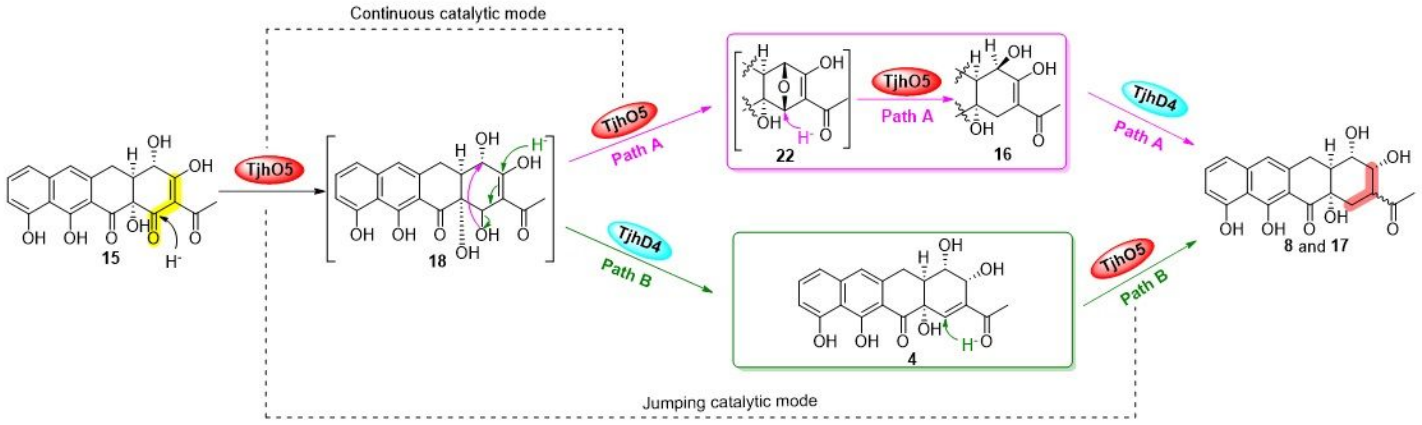

Figure 6

Proposed biosynthetic pathways (path A and path B) of multi-reduced modification by TjhO5 and TjhD4. The pink arrow and green arrow represent the steps of path A and B, respectively.

Supplementary Files

This is a list of supplementary files associated with this preprint. Click to download.

- O5D4SINCOMM.pdf
- graphicalabstract.jpg